Reaction–diffusion model of hair-bundle morphogenesis

Adrian Jacobo[a,b] and A. J. Hudspeth[a,b,1]

[a]Howard Hughes Medical Institute and [b]Laboratory of Sensory Neuroscience, The Rockefeller University, New York, NY 10065

Contributed by A. J. Hudspeth, September 12, 2014 (sent for review July 28, 2014)

The hair bundle, an apical specialization of the hair cell composed of several rows of regularly organized stereocilia and a kinocilium, is essential for mechanotransduction in the ear. Its precise organization allows the hair bundle to convert mechanical stimuli to electrical signals; mutations that alter the bundle's morphology often cause deafness. However, little is known about the proteins involved in the process of morphogenesis and how the structure of the bundle arises through interactions between these molecules. We present a mathematical model based on simple reaction–diffusion mechanisms that can reproduce the shape and organization of the hair bundle. This model suggests that the boundary of the cell and the kinocilium act as signaling centers that establish the bundle's shape. The interaction of two proteins forms a hexagonal Turing pattern—a periodic modulation of the concentrations of the morphogens, sustained by local activation and long-range inhibition of the reactants—that sets a blueprint for the location of the stereocilia. Finally we use this model to predict how different alterations to the system might impact the shape and organization of the hair bundle.

auditory system | development | hair cell | Turing pattern | vestibular system

Hair cells, which occur in the sensory epithelia of hearing and balance organs of vertebrates, are responsible for mechanotransduction in the inner ear. The specialized mechanoreceptive organelle of each such cell, the hair bundle, is a cluster of 10–300 actin-filled cylinders called stereocilia (1) that occur in a hexagonal pattern on a well-defined, bounded region of the apical cellular surface (Fig. 1). The stereocilia display a monotonic gradient in length along one of the hexagonal axes; at the tall edge stands a single true cilium termed the kinocilium. The mechanical forces initiated by sounds or movements owing to accelerations deflect the hair bundle, bending the stereocilia at their bases. This deflection opens ion channels located at the stereociliary tips and depolarizes the cell, transducing a mechanical stimulus into an electrical output.

The process of hair-bundle morphogenesis starts after a prospective hair cell has differentiated from a population of precursors (2–5). The kinocilium migrates from the center of the apical surface to one edge, providing the first morphological evidence of planar polarity. Microvilli on the apical surface then grow into stereocilia and establish the height gradient of the hair bundle. The numbers, positions, and lengths of the stereocilia are well controlled, producing consistent bundle shapes. In different individuals of the same species the number and dimensions of the stereocilia at a specific location of the cochlea vary by less than 5% (3). A hair bundle is accordingly among the most precisely specified organelles in a vertebrate organism.

The structure of the hair bundle, the basic features of which are similar in the organs of all vertebrate species, is essential for its proper functioning as a mechanotransducer. Of the hundreds of mutations that produce deafness in humans, approximately half affect the hair bundle (6, 7). Many of these mutations alter the normal development of hair cells and produce misoriented or misshapen bundles (6, 8–10). Although the effort to understand the molecular mechanisms of hair-bundle morphogenesis has led to the identification of several proteins involved in the process (9–11), we lack a theoretical understanding of how the precise shapes of hair bundles result from interactions among these molecules.

In this paper we propose a reaction–diffusion model to explain how the characteristic arrangement of stereocilia emerges through the formation of a Turing pattern (12). A Turing pattern is a spatial arrangement of molecules with a characteristic periodicity that arises and is maintained by a combination of local activation and long-range inhibition between those molecules. The pattern appears autonomously and independently of any preexisting positional information, with a characteristic period determined by the interplay between the rates of diffusion and reaction (13). With this model we examine how the boundaries of the bundle are delimited, how the hexagonal pattern of stereocilia is established, and how the gradient in height is determined.

Description of the Model

Our model is related to a system that was first studied as the simplest way known to produce oscillatory chemical reactions (14). When the spatiotemporal properties of this system were investigated, it was shown to display spatial patterns (15). The model describes the dynamics of two morphogens, U and V, that are synthesized from two substrates, A and B (Fig. 2*A*). Although "morphogen" often refers to molecules that produce signals at the tissue scale (16), we use the term in a broad sense applicable at the intracellular level. The reaction mechanism is

$$A \underset{k_{-1}}{\overset{k_1}{\rightleftharpoons}} U, \quad B \overset{k_2}{\rightarrow} V, \quad 2U + V \overset{k_3}{\rightarrow} 3U. \qquad [1]$$

Two molecules of U react with one molecule of V to create an additional molecule of U. This autocatalytic reaction creates a positive feedback loop, a common component of regulatory networks (17). V is considered to be stable and does not decay on

Significance

Our senses of hearing and balance rest upon the activity of hair cells, the ear's sensory receptors. Each hair cell detects mechanical stimuli with its hair bundle, an organelle comprising 10–300 cylindrical, actin-filled stereocilia. A bundle's structure is highly stereotyped: the stereocilia stand erect in a regular, hexagonal array and display a monotonic gradient in length along one axis. This precise organization is key to the operation of the hair bundle: mutations that disturb the morphology of the bundle generally result in deafness. Here we provide a detailed mathematical model of hair-bundle morphogenesis that reproduces the essential features of bundles. The model also permits prediction of the effects of mutations, some of which have already been observed.

Author contributions: A.J. and A.J.H. designed research; A.J. performed research; A.J. analyzed data; and A.J. and A.J.H. wrote the paper.

The authors declare no conflict of interest.

Freely available online through the PNAS open access option.

[1]To whom correspondence should be addressed. Email: hudspaj@rockefeller.edu.

This article contains supporting information online at www.pnas.org/lookup/suppl/doi:10.1073/pnas.1417420111/-/DCSupplemental.

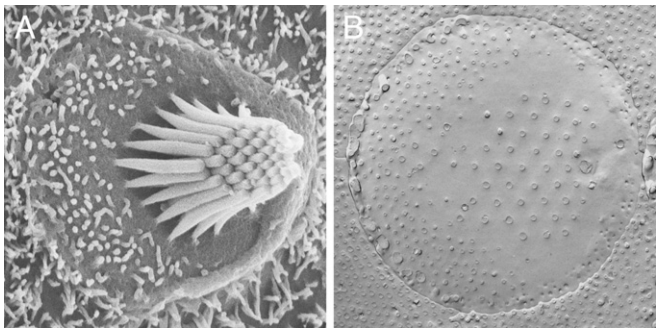

Fig. 1. (*A*) Scanning electron micrograph of a hair bundle protruding from the apical surface of a bullfrog's saccular hair cell. The bundle is formed by about 60 stereocilia of lengths increasing from left to right. At the tall edge of the bundle stands the kinocilium. (*B*) Freeze-fracture image of the apical surface of a hair cell from the same organ. The anchoring sites of the stereocilia can be seen in their characteristic hexagonal arrangement. The insertion point of the kinocilium and the cell's circumference are also visible.

the relevant timescales of the system, whereas U can decay back to A. Each of these components could in reality represent multiple molecules, but for the sake of simplicity we consider them as single entities.

We assume that U and V are diffusible. Because hair-bundle morphogenesis occurs at the apical surface of the cell (10), we consider that the molecules in our model diffuse laterally only at or within the membrane (18, 19), restricting the problem to two dimensions. We can write a set of equations to describe the dynamics of these morphogens and, by rescaling (*SI Appendix*, Section 1), reduce the number of parameters to yield the nondimensionalized equations

$$\begin{aligned}\frac{\partial u}{\partial t} &= \gamma\left(a - u + u^2 v\right) + d_u \nabla^2 u,\\ \frac{\partial v}{\partial t} &= \gamma\left(b - u^2 v\right) + d_v \nabla^2 v.\end{aligned} \qquad [2]$$

Here a, b, u, and v are the dimensionless concentrations of the respective chemical species. Throughout the text we refer to the chemical species with uppercase letters and to their concentrations with lowercase letters. γ is a reaction-rate coefficient; d_u and d_v are diffusion coefficients (15). Because the problem is two-dimensional, $\nabla^2 = \partial^2/\partial x^2 + \partial^2/\partial y^2$. We also assume that the morphogens cannot diffuse beyond the cell: the boundaries are reflecting.

We first consider the behavior of this system when the concentrations of the substrates are homogeneous. A necessary condition for the formation of patterns is then $d_v > d_u$ (15). If there were no diffusion, the system would reside at a steady state. If the concentration of U were to increase temporarily then the concentration of V would decrease, leading in turn to a decrease in the concentration of U and returning the system to the steady state. If we now consider diffusion, however, a decrease in v as a result of an increase in u would result in a net flux of V from neighboring regions, in turn causing u to drop in those regions and allowing v to exceed its steady-state value. A pattern would then be established with areas of high concentrations of U and low concentrations of V and vice versa. Regions of high concentration of U would be sustained by the autocatalytic reaction, which acts locally, but also thanks to the influx of V from neighboring regions, a mechanism that provides long-range inhibition (Fig. 2*A*). Even if the system exhibited a stable steady state in the absence of diffusion, this physical process would therefore destabilize the steady state and produce a pattern.

We can now construct a phase diagram for the behavior of the morphogens as a function of a and b (Fig. 2*B* and *SI Appendix*, Fig. S1) (20). When both a and b are small, the concentrations of the morphogens oscillate in time but are spatially homogeneous. For high concentrations of the substrates, u and v are stationary and homogeneous. Finally, for intermediate values of a and b, the morphogens U and V display a spatial pattern of concentrations. For large values of a the pattern is hexagonal. Otherwise there is bistability between hexagonal and stripe patterns, in which case the final state adopted by the system depends on the initial spatial distributions and concentrations of U and V.

Formation of Hexagonal Patterns

We propose that developing hair cells tune the spatial concentrations of a and b to create a region where u and v produce a hexagonal pattern. This region corresponds to the extent of the hair bundle, within which the hexagonal pattern constitutes a blueprint for the nucleation of stereocilia. The problem now becomes finding a way for the cells to establish the correct spatial profiles for the substrates. The simplest assumption is that distinct parts of the cell act as sources for A and B and that these molecules can diffuse while they decay at specific rates. This model is described by

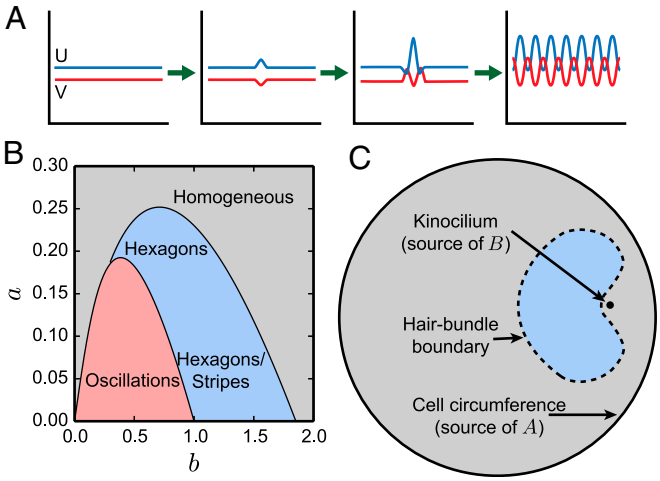

Fig. 2. (*A*) Schematic illustration of the pattern-formation process. The morphogens U and V start with homogeneous concentrations. When a random fluctuation causes a local increase in u, it will in turn produce a decrease of v at the same location. Given its fast diffusion, V will be depleted from the surroundings of the perturbation, reducing u at those locations. This process has a characteristic wavelength and sets a distribution of peaks and valleys in the morphogens' concentrations, known as a Turing pattern. (*B*) Phase diagram in which the possible arrangements of the morphogens are shown as functions of the concentrations of the substrates. For low values of a and b the concentrations of the morphogens oscillate in time (red area). For high concentrations of the substrates the morphogens adopt homogeneous and stationary concentrations (gray area). For intermediate values of a and b the morphogens form a Turing pattern (blue area). The pattern can involve either hexagons or stripes, depending on the concentrations of the substrates and the initial conditions of the morphogens (20). $\gamma = 10{,}000$, $d_u = 0.8$, and $d_v = 16$. (*C*) Diagram of the apical surface of a hair cell. The circumference of the cell and the kinocilium act as sources of the substrates. The concentration of each substrate decreases with distance from its source, creating gradients across the apical surface of the cell. The combination of these two gradients locally changes the stability of the morphogens delimiting the boundary of the hair bundle. The colors in each area correspond to those of *B* and show the different solutions the morphogens take at each position of the cell. In the gray area the morphogens reach a spatially homogeneous configuration. Inside the blue region the morphogens form a hexagonal pattern that acts as a blueprint for the location of the stereocilia.

$$\frac{\partial a}{\partial t} = d_a \nabla^2 a - k_a a,$$
$$\frac{\partial b}{\partial t} = d_b \nabla^2 b - k_b b, \qquad [3]$$

in which d_a and d_b are the diffusion constants of the respective substrates and k_a and k_b their rate constants for decay. A and B have sources with shapes $S_a(x,y)$ and $S_b(x,y)$ at which the values of a and b are fixed, respectively, to a_0 and b_0 (Fig. 2*C*). These two values represent the expression levels of A and B. We assume again that the diffusion of the substrates is two-dimensional and that the boundaries are reflecting. Following the prescribed dynamics, the concentrations of A and B reach a steady state with gradients of concentration declining from the sources (Fig. 3). Substrate gradients then convey positional information, acting as rulers by setting distances. Although this arrangement is analogous to the French Flag Model for tissue patterning (21), in our case the gradients are used to produce patterns within an individual cell instead of across many cells.

Because the shape and orientation of a hair bundle are related to the position of the kinocilium and basal body (9), it is reasonable to suppose that one of the sources is located there. Furthermore, when the kinocilium is situated near the cell's boundary, stereocilia develop only toward the center of the cell and never in the narrow region between the kinocilium and the edge of the cell (Fig. 1*B*). This broken symmetry suggests that the boundary acts as a source for one of the substrate molecules. Using this information and calculating the predicted shape of the bundle for different locations of the sources (*SI Appendix*, Figs. S2 and S3), we found that reproducing the boundary of a normal bundle requires that the source of A be located at the circumference of the cell and the source of B at the kinocilium (Fig. 2*C*). Only a single source, either at the kinocilium or at the boundary, does not reproduce the shape of the hair bundle: both sources are required.

With these particular sources the dynamics for the substrates can evolve until the intracellular gradients of a and b reach a steady state. Each point at the apical surface of the cell is then characterized by its corresponding values of a and b. Using the phase diagram we can relate this pair of values (Fig. 2*B*) to the different solutions of the system. By repeating this procedure at each point on the surface of the cell we can calculate the approximate shape of the region where the hexagonal pattern is stable (*SI Appendix*, Section 1.1). This region will act as a blueprint for the formation of the hair bundle.

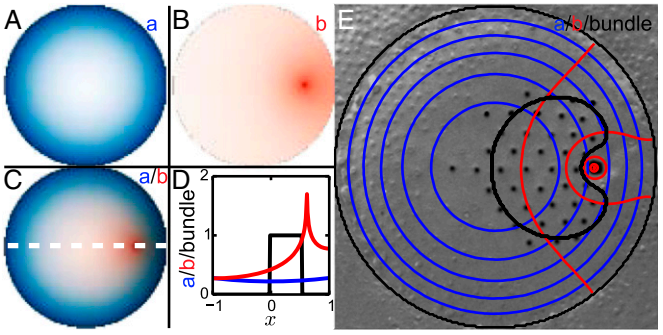

Fig. 3. (*A*–*C*) Expression patterns of substrates A (blue) and B (red). The concentrations of the substrates are highest at their respective sources and decline with distance from those sources. (*D*) The concentration of each of the substrates is shown along the white dashed line in *C*. From the values of a and b at each point one can determine, by means of the phase diagram (Fig. 2*B*), the corresponding behavior of the morphogens in different regions of the cell's apical surface. Then the approximated area for the formation of a hexagonal pattern can be delimited (black), with its boundary corresponding to the edge of the bundle. (*E*) Isoconcentration lines of a (blue) and b (red) overlaid on a freeze-fracture image of a hair bundle, with the locations of the stereocilia enhanced (black dots). The black line marks the edge of the bundle as predicted by the phase diagram (Fig. 2*B*). $a_0 = 0.28$, $b_0 = 1.7$, $d_a = d_b = 1$, and $k_a = k_b = 1$.

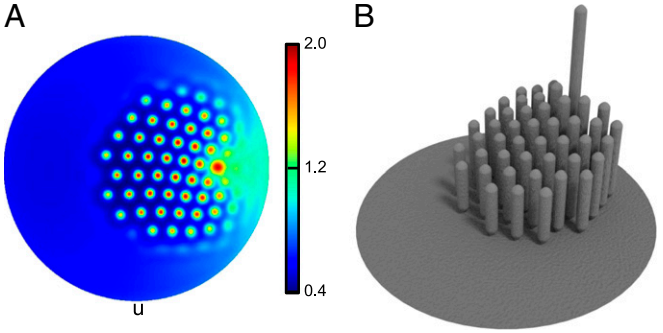

Fig. 4. (*A*) Expression pattern of U created by the substrate gradients in Fig. 3. The morphogens form a hexagonal pattern within the area of a hair bundle. (*B*) Rotated view of a 3D reconstruction of the hair bundle, derived from the blueprint shown in *A*. The concentration peaks of U specify the locations of stereocilia whose lengths are proportional to the concentration of A. The length of the kinocilium is arbitrary and not predicted from the model. Parameter values are $\gamma = 10{,}000$, $d_u = 0.8$, and $d_v = 16$.

Comparing the calculated stability regions to freeze-fracture images of actual hair bundles, we can obtain a set of parameter values for the substrate gradients that reproduces the shape of a typical bundle. The concentration of A exhibits a gradient decreasing from the circumference toward the center of the cell (Fig. 3). Near the boundary of the cell a is high and corresponds to a homogeneous concentration of the morphogen (Fig. 2*B*). Toward the center of the cell the concentration of A decreases and reaches the hexagon-formation region in the phase diagram, allowing the appearance of a bundle. The concentration of B decreases analogously with distance from the kinocilium (Fig. 3). Near the kinocilium b corresponds to the region of hexagon formation, whereas near the center of the cell its value declines and the expression of the morphogens becomes homogeneous. Because each substrate can by itself yield only bundles that follow its isoconcentration contours (Fig. 3*E*), producing a correctly shaped bundle requires at least two substrates originating at distinct sources.

Using the expression patterns for A and B we can simulate the dynamics of the morphogens (Eq. **2**), which are produced from the substrates and self-organize to specify a blueprint for the location of stereocilia (Fig. 4*A*). The concentrations of U and V show spots that are organized in a hexagonal pattern. The concentration of U is higher than average at these spots, whereas the concentration of V is lower than average. At these spots, where u reaches a certain threshold, a signaling cascade can nucleate a stereocilium. In addition, if the rate of stereociliary elongation is proportional to a, we can obtain a height gradient for the stereocilia that qualitatively matches that in an actual bundle (Fig. 4*B*). This result suggests a relationship between the shape of the bundle's edge and its height gradient.

We have assumed that the substrate concentrations evolve on a timescale much faster than that governing the morphogen concentrations. This distinction is reflected in the fact that the substrate gradients are considered constant in time in the equations for the morphogens (Eq. **2**), an assumption that simplifies calculations and does not significantly alter the results. Starting from random initial conditions, a and b evolve until they form stationary gradients. The morphogens are produced from the substrates without altering these gradients and the blueprint for the bundle results. The substrates in effect act as spatially varying parameters in the morphogen equations.

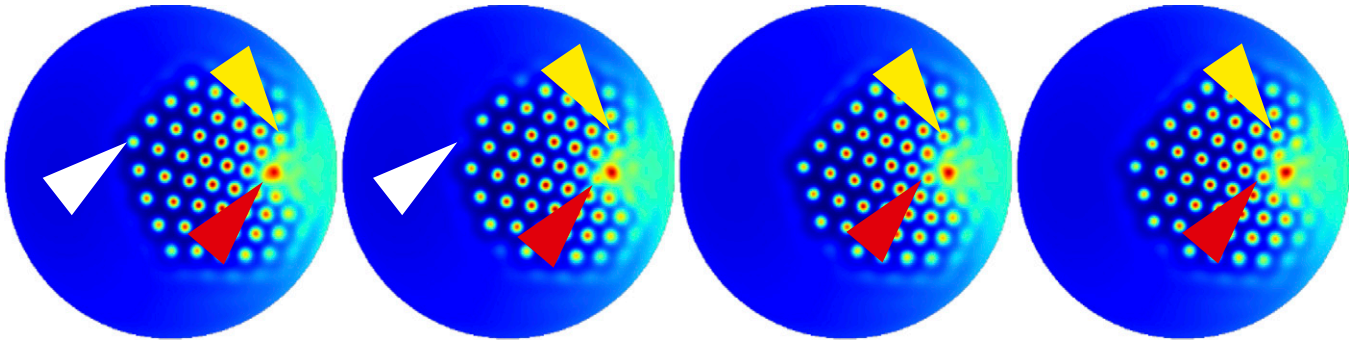

Fig. 5. Temporal evolution of U. Due to the gradient in the substrate concentrations the pattern drifts toward the center of the cell. New spots are created at the tall edge of the bundle (yellow arrowheads) and at the kinocilium (red arrowheads). Spots are destroyed when they reach the short edge of the bundle (white arrowheads). The first image corresponds to $t = 2.925 \times 10^{-3}$ and each successive frame is separated by $\delta t = 9 \times 10^{-4}$. The parameter values and substrate gradients are the same as in Fig. 4.

Movement of Hexagonal Patterns

Turing patterns with gradients in the parameter values characteristically drift along the gradients (22) and this is the case for our system. Starting from random initial conditions, u and v rapidly form a hexagonal pattern within the bundle region; then, on a much slower timescale, the pattern slides toward the center of the cell with new spots arising near the circumference and old spots evaporating near the center (Fig. 5 and Movie S1). The disappearance of spots breaks the hexagonal arrangement of the pattern, leaving isolated stereocilia at the edge of the bundle. Such isolated stereocilia are characteristic of actual hair bundles (Fig. 3*E*).

The stereocilia of actual bundles display two distinct alignments with respect to the kinocilium (23). In one of these configurations, a line that bisects the apical surface and passes through the kinocilium (Fig. 3*C*) is parallel to successive rows of stereocilia (Fig. 1*B*). In the other configuration the rows of stereocilia form an angle of 30° with respect to this line. The concentration peak of B at the kinocilium acts as a localized source of spots (24) that change the alignment of the pattern as they are created. Depending on the initial conditions for the morphogens, we observe these two arrangements during the evolution of the pattern. We have not studied systematically the conditions for each to appear.

The dynamic nature of the pattern poses the question of how this information might be used to create a stationary blueprint for the stereocilia. The time required for the pattern to drift one wavelength greatly exceeds that involved in pattern formation. If the timescale for stereociliary nucleation is also short compared with that for drifting, the developing cell would encounter a quasi-stationary pattern and the drift would not pose a problem. Another possibility is that, after the pattern has formed, downstream molecules read the concentration of the pattern at a specific time, creating a "frozen" blueprint that can be used to nucleate stereocilia at their correct positions.

Predictions of the Model

Having reproduced the shape of a typical vestibular hair bundle, we can now predict the effects of different alterations to the system. These perturbations might model the actions of specific mutations.

By altering the diffusion coefficients d_u and d_v of the morphogens we can change the number and separation of the stereocilia or eliminate their hexagonal pattern altogether. The changes could be accomplished by adjusting the size of the molecules U and V or their binding to cellular constituents, thereby changing their effective diffusion coefficients. If the diffusion coefficients of both morphogens decrease proportionally, the distance between stereocilia declines, so one should observe additional stereocilia in a more tightly packed hexagonal pattern. If the separation of stereocilia becomes comparable to their diameters it is expected that one would encounter fused stereocilia.

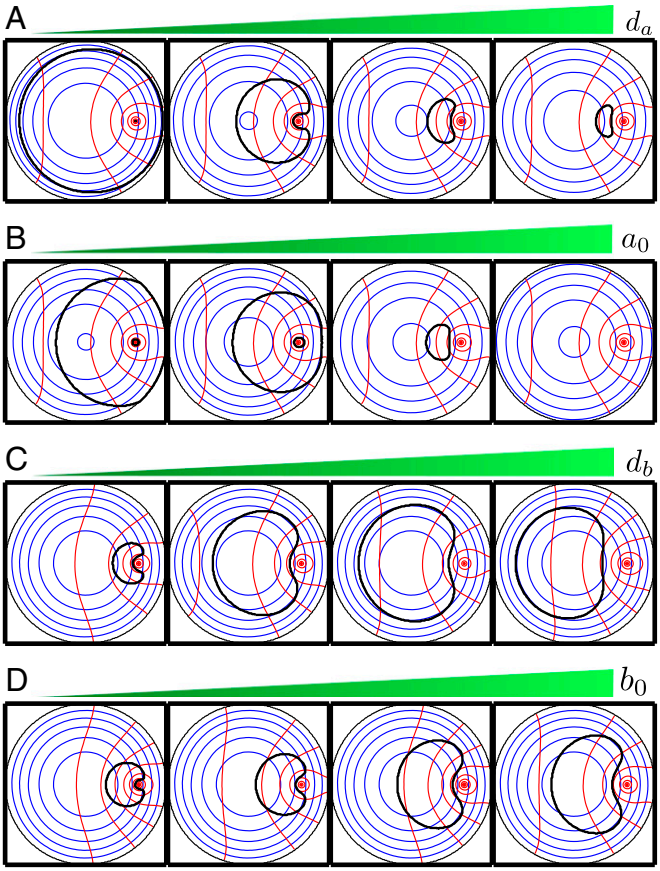

Fig. 6. (*A–D*) Isoconcentration curves for the substrates A (blue) and B (red) and approximated shapes of the predicted hair bundles (black) as functions of the parameter values. (*A*) Increasing the value of d_a reduces the area of the hair bundle (from left to right d_a = 0.1, 0.8, 1.5, and 1.7). (*B*) Changing the expression level a_0 at the source has a similar effect on the area of the bundle (from left to right a_0 = 0.24, 0.26, 0.3, and 0.32). (*C*) Raising the diffusion coefficient d_b increases the area of the stereociliary cluster, while moving it away from the kinocilium (from left to right d_b = 0.5, 1.5, 2, and 3). (*D*) Changes in b_0 have a similar effect on the area of the bundle, but only a small effect on its position with respect to the kinocilium (from left to right b_0 = 1.3, 1.5, 1.9, and 2.1). In all panels the remaining parameters have the same values as in Fig. 3.

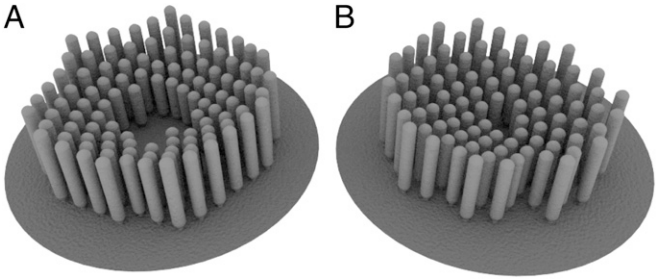

Fig. 7. Predicted bundle shapes for centered kinocilia. We calculate the concentration gradients of the substrates when the kinocilium is located at the center of the cell. We also assume that the level of expression of *B* is altered from that in normal hair bundles. (*A*) Stereocilia grow in an annulus, leaving a bare region near the kinocilium ($b_0 = 0.3$). (*B*) Stereocilia grow in a circle, leaving almost no empty space around the kinocilium ($b_0 = 0.21$). For both images $a_0 = 0.28$, $d_a = d_b = 1$, and $k_a = k_b = 1$.

One requisite for the formation of a hexagonal pattern is that *V* diffuses much faster than *U*. As the ratio between the diffusion coefficients of *V* and *U* decreases, the region of pattern formation in the phase space shrinks. At some point the values of *a* and *b* along their gradients no longer traverse the pattern-formation region and the blueprint for the bundle vanishes. It is beyond the scope of our model to predict the appearance of the resultant bundle in this case.

Modifying the expression patterns of the substrates should change the overall shape of the bundle. We can calculate the intracellular gradients of the substrates and the corresponding boundaries of the hair bundles for different values of the parameters (Fig. 6). Because we are concerned with only the steady-state values of *a* and *b*, the relevant parameters are the diffusion constants d_a and d_b and the expression levels a_0 and b_0 (*SI Appendix*, Section 2). If the diffusion constant of *A* is increased, the area of the bundle should decrease; for a great enough increment the bundle should disappear. On the contrary, if d_a decreases, the bundle's area should increase and, for small enough values of this parameter, stereocilia should appear in the narrow region between the kinocilium and the cell circumference. Similar effects are achieved by changing the production rate of *A*. Increasing the diffusion constant of *B* has the opposite effect, increasing the area of the bundle while simultaneously moving the stereociliary cluster away from the kinocilium. If the expression level of *B* rises sufficiently it should be possible to observe clusters of stereocilia that are detached from the kinocilium. Raising the production rate of *B* also increases the area of the bundle without moving it substantially.

Mutations of the genes that control the formation of the kinocilium alter the shape of hair bundles in the mammalian cochlea. Inactivation of the intraflagellar-transport gene *ift88* or *kif3a* affects the development and subsequent migration of the kinocilium (9). Cells with centrally positioned basal bodies or kinocilia display annular or circular hair bundles. Treatment of developing hair cells with pertussis toxin also alters the peripheral migration of the kinocilium and produces circular bundles (10). Upon locating the kinocilium at the center of the cell and slightly increasing the expression of *B*, our model can reproduce circular or annular bundles (Fig. 7) and thus predicts that these phenotypes can arise in vestibular hair cells. Considering the extensive differences between the shapes of cochlear and vestibular bundles, the experimental observation of similarly shaped bundles in the cochleae and utricles of mutant animals would support the ideas behind our model. Our model implies that a hair bundle's boundary is related to its height gradient, and therefore predicts that these two types of bundles have stereocilia of decreasing lengths toward the center of the cell.

Discussion

We have presented a model of how substrates and morphogens interact to create the shape and arrangement of a hair bundle. Given that the molecular details of hair-bundle morphogenesis are unknown, we worked with the minimal number of molecular constituents and the simplest interactions between them. Similar results can be obtained with more complex versions as long as the key features of the model remain. The essential ingredients are a set of substrate molecules that can convey positional information from the cell circumference and the kinocilium and a set of morphogens that change stability depending on the substrate concentrations to form a hexagonal Turing pattern. Although our model invokes diffusion to transport molecules within the cell, active transport or a combination of active and diffusive transport can yield similar results.

Two molecular complexes involved in the morphogenesis of hair bundles have been shown to form complementary expression domains with decreasing concentration gradients from the cell circumference toward the center (10, 11). The expression patterns of mInsc/LGN/Gαi and aPKC/Par-3/Par-6b are correlated with a bundle's shape. Considering each of these two complexes as a single entity produces in vestibular hair cells a pattern of expression that is compatible with that of *A* in the model (10).

To the best of our knowledge there are no reported proteins that show an expression pattern that matches that of *B*. However, the primary cilium of the cell represents a nexus for signaling pathways during development across many different cell types (25) and there is a well-established relationship between the location of the kinocilium and the shape and orientation of the bundle (9, 10). These observations are strong indications that the kinocilium acts as a signaling center for hair-bundle development and that a molecule corresponding to *B* exists.

Stereocilia consist primarily of densely packed actin filaments enclosed by the cell membrane. Because the pattern created by the morphogens serves as a blueprint for the location of stereocilia, at least one of these molecules is expected to be an upstream regulator of the actin network. One protein that might play this role and is also involved in the establishment of planar cell polarity is Cdc42. In *Drosophila* this molecule interacts with Par proteins and aPKC to regulate the actin cytoskeleton (26). In yeast the active and inactive forms of Cdc42 form a Turing pattern that creates a bud before cell division (27–29). The active and inactive forms of Cdc42 are accordingly candidates to be the morphogens *U* and *V* in our model.

If the tip links that connect successive rows of stereocilia are removed by chelation of Ca^{2+} the stereocilia in shorter rows shrink (30). Moreover, if the proteins that compose the tip links are deficient, the length of the stereocilia is disrupted (31). These observations suggest a mechanical feedback between successive rows of stereocilia that contributes to the height gradient, in addition to the mechanism proposed here. Molecules like harmonin-b, myosin VIIa, whirlin, and myosin XVa (31–33) are required to obtain a proper height gradient and could be downstream effectors of the proposed mechanism.

We were unable by simple extensions of our model to reproduce the characteristic "W" shape of hair bundles from outer hair cells. This suggests that cochlear bundles require additional mechanisms not present in other organs. Comparing the molecular components of cochlear and vestibular hair bundles in mammals may therefore provide information about these additional mechanisms and help explain how the shape of hair bundles is controlled.

In our model we do not explicitly consider the role of external signals from other hair cells or supporting cells in the establishment of the bundle. Mutant mice deficient in nectin-3, a cell-adhesion protein expressed only in supporting cells, display disturbances in the orientation and morphology of their hair bundles (34). This result suggests that the morphogenetic process

is not cell-autonomous but requires signals from the surrounding cells. A simple way of accounting for these signals in our model could be by a modulation of the gradient of a, more precisely by considering that intercellular signaling sets the value of a_0 and alterations to these signals change this value and therefore affect the shape of the hair bundle.

The interactions between the proteins mentioned above are more complex than those in our model. As the actual morphogenetic proteins are identified by experiments, the model should be updated to include a more complete interaction network and measured values for the rate and diffusion coefficients. These refinements will permit a more quantitative comparison between model and experiment. This extension may also allow reproduction of the shape of hair bundles in the mammalian cochlea, a task beyond the scope of this simple model. Finally, future work should evaluate the effects of random fluctuations on the system, especially regarding the establishment of the height gradient across the bundle.

Materials and Methods

Calculations are described in *SI Appendix*. Using a finite-volume method, we solved Eqs. **2** and **3** with the software library FiPy (35).

ACKNOWLEDGMENTS. We thank the members of our research group for constructive comments on the manuscript. A.J. is a Research Associate and A.J.H. is an Investigator of Howard Hughes Medical Institute.

1. Hudspeth AJ (2008) Making an effort to listen: Mechanical amplification in the ear. *Neuron* 59(4):530–545.
2. Cotanche DA, Corwin JT (1991) Stereociliary bundles reorient during hair cell development and regeneration in the chick cochlea. *Hear Res* 52(2):379–402.
3. Tilney LG, Tilney MS, DeRosier DJ (1992) Actin filaments, stereocilia, and hair cells: How cells count and measure. *Annu Rev Cell Biol* 8:257–274.
4. Denman-Johnson K, Forge A (1999) Establishment of hair bundle polarity and orientation in the developing vestibular system of the mouse. *J Neurocytol* 28(10-11): 821–835.
5. Frolenkov GI, Belyantseva IA, Friedman TB, Griffith AJ (2004) Genetic insights into the morphogenesis of inner ear hair cells. *Nat Rev Genet* 5(7):489–498.
6. Richardson GP, de Monvel JB, Petit C (2011) How the genetics of deafness illuminates auditory physiology. *Annu Rev Physiol* 73:311–334.
7. hereditaryhearingloss.org/. Accessed May 19, 2014.
8. Ross AJ, et al. (2005) Disruption of Bardet-Biedl syndrome ciliary proteins perturbs planar cell polarity in vertebrates. *Nat Genet* 37(10):1135–1140.
9. Jones C, et al. (2008) Ciliary proteins link basal body polarization to planar cell polarity regulation. *Nat Genet* 40(1):69–77.
10. Ezan J, et al. (2013) Primary cilium migration depends on G-protein signalling control of subapical cytoskeleton. *Nat Cell Biol* 15(9):1107–1115.
11. Tarchini B, Jolicoeur C, Cayouette M (2013) A molecular blueprint at the apical surface establishes planar asymmetry in cochlear hair cells. *Dev Cell* 27(1):88–102.
12. Turing AM (1952) The chemical basis of morphogenesis. *Philos. Trans R Soc Lon Ser B* 237(641):37–72.
13. Kondo S, Miura T (2010) Reaction-diffusion model as a framework for understanding biological pattern formation. *Science* 329(5999):1616–1620.
14. Schnakenberg J (1979) Simple chemical reaction systems with limit cycle behavior. *J Theor Biol* 81:389–400.
15. Murray JD (2003) *Mathematical Biology. II: Spatial Models and Biomedical Applications* (Springer, New York), 3rd Ed.
16. Kicheva A, Cohen M, Briscoe J (2012) Developmental pattern formation: Insights from physics and biology. *Science* 338(6104):210–212.
17. Fall CP, Marland ES, Wagner JM, Tyson JJ, eds (2002) *Computational Cell Biology* (Springer, New York), 1st Ed.
18. Alberts B, et al. (2008) *Molecular Biology of the Cell* (Garland Science, New York), 5th Ed.
19. Ramadurai S, et al. (2009) Lateral diffusion of membrane proteins. *J Am Chem Soc* 131(35):12650–12656.
20. Dufiet V, Boissonade J (1992) Numerical studies of Turing patterns selection in a two-dimensional system. *Phys A Stat Mech* 188:158–171.
21. Wolpert L (1969) Positional information and the spatial pattern of cellular differentiation. *J Theor Biol* 25(1):1–47.
22. Page KM, Maini PK, Monk N A M (2005) Complex pattern formation in reaction-diffusion systems with spatially varying parameters. *Physica D* 202:95–115.
23. Rowe MH, Peterson EH (2004) Quantitative analysis of stereociliary arrays on vestibular hair cells. *Hear Res* 190(1-2):10–24.
24. Parra-Rivas P, Gomila D, Matías MA, Colet P (2013) Dissipative soliton excitability induced by spatial inhomogeneities and drift. *Phys Rev Lett* 110(6):064103.
25. Goetz SC, Anderson KV (2010) The primary cilium: A signalling centre during vertebrate development. *Nat Rev Genet* 11(5):331–344.
26. Leibfried A, Müller S, Ephrussi A (2013) A Cdc42-regulated actin cytoskeleton mediates Drosophila oocyte polarization. *Development* 140(2):362–371.
27. Altschuler SJ, Angenent SB, Wang Y, Wu LF (2008) On the spontaneous emergence of cell polarity. *Nature* 454(7206):886–889.
28. Goryachev AB, Pokhilko AV (2008) Dynamics of Cdc42 network embodies a Turing-type mechanism of yeast cell polarity. *FEBS Lett* 582(10):1437–1443.
29. Kozubowski L, et al. (2008) Symmetry-breaking polarization driven by a Cdc42p GEF-PAK complex. *Curr Biol* 18(22):1719–1726.
30. Rzadzinska AK, Schneider ME, Davies C, Riordan GP, Kachar B (2004) An actin molecular treadmill and myosins maintain stereocilia functional architecture and self-renewal. *J Cell Biol* 164(6):887–897.
31. Lefèvre G, et al. (2008) A core cochlear phenotype in USH1 mouse mutants implicates fibrous links of the hair bundle in its cohesion, orientation and differential growth. *Development* 135(8):1427–1437.
32. Mburu P, et al. (2003) Defects in whirlin, a PDZ domain molecule involved in stereocilia elongation, cause deafness in the whirler mouse and families with DFNB31. *Nat Genet* 34(4):421–428.
33. Delprat B, et al. (2005) Myosin XVa and whirlin, two deafness gene products required for hair bundle growth, are located at the stereocilia tips and interact directly. *Hum Mol Genet* 14(3):401–410.
34. Fukuda T, et al. (2014) Aberrant cochlear hair cell attachments caused by Nectin-3 deficiency result in hair bundle abnormalities. *Development* 141(2):399–409.
35. Guyer JE, Wheeler D, Warren JA (2009) FiPy: Partial differential equations with python. *Comput Sci Eng* 11:6–15.